Ligand binding to distinct states diverts aggregation of an amyloid-forming protein

Lucy A. Woods[#], Geoffrey W. Platt [#], Andrew L. Hellewell, Eric W. Hewitt, Steve W. Homans, Alison E. Ashcroft* & Sheena E. Radford*

Supplementary Methods

Assays for a colloidal mechanism of inhibition

Several small molecules have been shown to inhibit fibrillation *via* a colloidal mechanism. [1-4] To determine whether this is the case for rifamycin SV and β_2m under the conditions used (25 mM sodium phosphate, pH 2.5, 10% (*v/v*) DMSO or acetonitrile) rifamycin SV (1 mM) was allowed to equilibrate for 3 h through a 3000 Da cut-off membrane (Spectrapore) at 37 ºC and the amount of ligand able to pass through the membrane determined by the absorbance at 445 nm using an extinction coefficient of 14235 $M^{-1}cm^{-1}$. [5] The resulting material was then used in fibrillation assays as described in the Methods (main text). In addition, rifamycin SV (1 mM) was centrifuged for 30 min at 418,000x *g* and the supernatant used in fibrillation assays. Finally, the ability of 400 μM rifamycin SV to inhibit fibrillation of 40 μM β_2m in the presence of 5 $mgml^{-1}$ of BSA, [3] or to inhibit fibrillation of 69 μM α-synuclein in 25 mM sodium phosphate/sodium acetate pH 2.5 [6] was tested.

Preparation of fibrillation assays using α-synuclein

α-Synuclein was expressed from the plasmid pET23a into which a synthetic gene (purchased from MWG) encoding the human gene sequence (optimised for codon usage in *E.coli*) was introduced. Expression of the protein was obtained in *E.coli* BL21 DE3 cells using LB medium and inducing expression when the OD_{600} reached 0.6 absorbance units using 1 mM

IPTG. The protein was purified using acid precipitation [7] followed by anion exchange chromatography (HiTrap Q HP 5 ml, GE Healthcare), as described in [8]. Fibrillation of the protein (69 μM) was assayed in sodium phosphate/sodium acetate, pH 2.5 at 37 ºC with agitation at 200 rpm. After an incubation time of 72 h, the presence of fibrils was determined by TEM and through analysis of soluble protein remaining after centrifugation of the sample for 30 min at 16,300x *g* by SDS-PAGE.

Depolymerization assays

Amyloid-like fibrils were assembled from 45 μM β_2m in 25 mM sodium acetate / 25 mM sodium phosphate (pH 2.5), 0.04 % (*w/v*) NaN_3 and 10 % (*v/v*) DMSO. TEM confirmed the presence of LS fibrils. The fibrils were distributed into 95 μl aliquots in a 96-well plate and incubated at 37 °C, 200 rpm. At various times (0 - 311 h), 5 μl of DMSO or 5 μl of 20 mM rifamycin SV in DMSO were added and fibril stability monitored subsequently using SDS-PAGE and TEM. All reactions were performed in triplicate.

Cell viability assays

For assays of cytotoxicity, SH-SY5Y or RAW 264.7 cells were incubated with β_2m samples (2.4 μM monomer or its equivalent) for 24 h at 37 °C in 5 % CO_2 before MTT cell viability assays were carried out as described previously. [9] The results were normalized using the signal for cells treated with buffer alone (or buffer containing 1 mM rifamycin SV in 10% (*v/v*) DMSO which was diluted 1:100 into the cell medium, as appropriate) (100 % viability) and cells treated with 0.1% (*w/v*) mM NaN_3 (0 % viability). Rifamycin SV has previously been shown to have no effect on cell viability of eukaryotic cells. [10]

Aging of rifamycin SV

Rifamycin SV is known to be unstable in solution [11]. To determine the oxidation status of the ligand in the fibril inhibition assays, ESI-MS was used to measure the mass of the ligand subsequent to incubation with 38 μM β_2m at pH 2.5 at 25 ºC. The MaxEnt algorithm, provided with the MassLynx software, [12] was used to convert the m/z values onto a mass scale revealing that the rifamycin species bound to β_2m immediately after dissolution (400 μM final concentration, 10% (*v/v*) acetonitrile) has a mass of 698 Da (Supplementary Figure S2a). This corresponds to a rifamycin SV species consisting of a reduced dihydroxy naphthylene group where no sodium ion is bound. ESI-MS analysis of 400 μM rifamycin SV incubated in 20 mM ammonium formate pH 2.5, 10% (*v/v*) acetonitrile indicated that rifamycin SV is oxidised to the quinone form, rifamycin S (696 Da), within 24 h of incubation (Supplementary Figure S2a). This molecule inhibits fibril formation albeit with reduced potency compared with its reduced counterpart (Supplementary Figure S1e). Oxidation of the small molecule has little effect on its ability to bind to different charge states of monomeric β_2m (Supplementary Figure S2b).

Ligand binding controls using ESI-MS

Two different control methods were used to determine whether binding between β_2m and rifamycin SV occurs during the process of ionisation, causing artefactual binding. The first method involved adding an excess of a second ligand. [13] Accordingly, 40 μM β_2m/ 40 μM rifamycin S/ 400 μM rifaximin was incubated in 10 mM ammonium formate at pH 2.5 and analysed by ESI-MS. The resulting spectra show that despite the presence of a ten-fold molar excess of rifaximin, rifamycin SV binding to all of the β_2m charge states can still be observed (Supplementary Figure S2c). This result shows that the β_2m/rifamycin SV complex is most likely to be formed in solution, as formation of a protein-ligand interaction upon droplet dehydration will favor the formation of the β_2m/rifaximin complex. Interestingly, binding of rifaximin to β_2m causes a shift in the equilibrium of co-existing β_2m monomeric conformers

towards more compact (less highly charged) states (Supplementary Figure S2c), consistent with binding in solution. The second control method to estimate the specificity of binding involves adding a second competitor protein. [14] In this experiment, horse heart myoglobin (40 μM) was incubated in stoichiometric amounts with β_2m and rifamycin SV. In this case, binding between β_2m and rifamycin SV is still observed, while no binding was detected between myoglobin and rifamycin SV (Supplementary Figure S2d). Together these control indicate that rifamycin SV binding to β_2m is unlikely to occur during the electrospray process.

Quantification of ESI mass spectra

To assign drift time signals to protein conformers and/or oligomers, the protocol described previously [15] was followed, in which the mean ion mobility arrival time for a particular ion is plotted against its charge state. This reveals three distinct conformational families of monomeric β_2m in addition to protein dimer, trimer and tetramer. Once assigned, each ion mobility arrival time distribution (ATD) for each charge state was isolated using Driftscope software supplied with the mass spectrometer and a centroided mass spectrum generated based on peak area to give a quantitative value. This procedure was repeated for each resolved ATD for each conformer/oligomer. For overlapping ATDs, Gaussian distributions were fitted using Microsoft Excel and were assigned a percentage of the total signal area. Centroided mass spectra for these overlapping ATDs were generated and a quantitative value assigned based on the signal percentage. A total protein ion count was calculated by summing each of the ATDs. Thus, the percentage contribution of each conformer or oligomer contributes to the total protein signal was calculated. All salt adducts (sodium and formate) associated with the protonated molecular ions were included when calculating the contributions of the ions. Where ligands were present, ligand bound protein peaks were also included in the contribution to each ion.

Supplementary Results

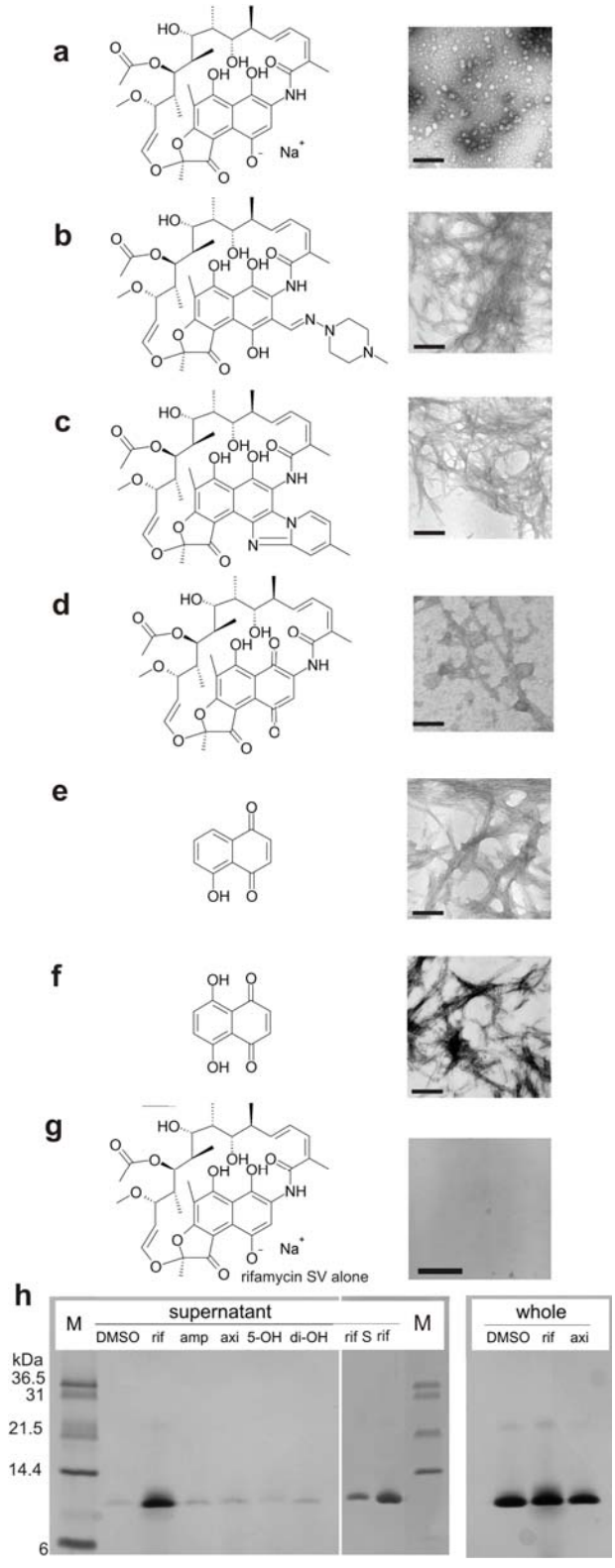

Supplementary Figure 1

Molecular structures of rifamycin SV and analogues alongside TEM images of the species

formed at the endpoint of incubation. **a** Rifamycin SV (rif), **b** rifampicin (amp), **c** rifaximin (axi), **d** rifamycin S (rif S), **e** 5-hydroxy-1,4-naphthoquinone (5-OH), **f** 5,8-dihydroxy-1,4-naphthoquinone (diOH) and **g** rifamycin SV alone (no β_2m). **h** SDS-PAGE showing the soluble material remaining after assembly is complete (48 h) (labeled supernatant) and the total protein concentration in each sample (labeled 'whole') for the reactions containing DMSO, rifamycin SV or rifaximin. All assays contained 45 μM β_2m and 1 mM small molecule and were incubated at pH 2.5, 25 ºC with agitation (600 rpm), as described previously [16]. The scale bar in each TEM image represents 200 nm.

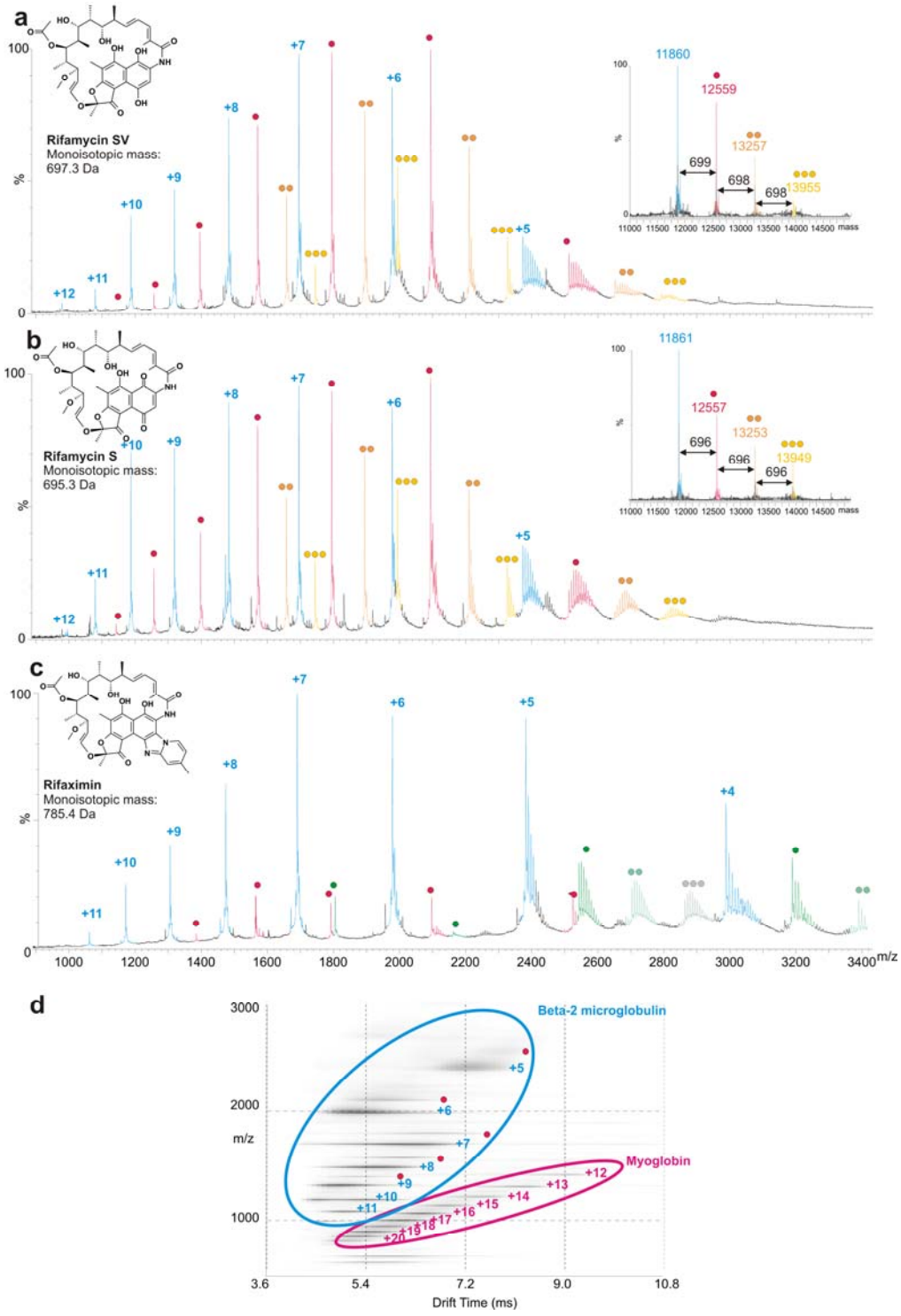

Supplementary Figure 2

Binding of rifamycin analogues to 38 μM β_2m shown using ESI-MS and ESI-IMS-MS. All spectra were acquired with a sampling cone voltage of 70V **a** 400 μM freshly dissolved rifamycin SV binds to each charge state of β_2m. The MaxEnt profile (inset) shows the mass of the bound ligand is 698±1 Da, consistent with binding of the reduced, sodium-free ligand. **b**

400 μM aged rifamycin SV binds to each charge state of β_2m. The MaxEnt profile (inset) shows that the mass of aged rifamycin SV is 696±1 Da, which corresponds to the oxidised quinone form, known as rifamycin S. In **a** and **b** the charge states colored blue result from ligand-free β_2m, red circles indicate 1:1 β_2m:ligand complexes and yellow circles indicate complexes with two or more ligands bound to each β_2m monomer. **c** ESI mass spectrum of β_2m incubated with a mixture of 40 μM rifamycin SV and 400 μM rifaximin. Rifamycin SV is observed to bind to all charge states, while rifaximin binds only to the charge states that arise from the more compact conformers, resulting in an increase in relative intensity of the +5 and +4 charge states compared with the charge states observed when rifamycin SV is added to β_2m. In this spectrum blue peaks identify ligand free monomeric β_2m, rifamycin SV-bound peaks are shown in red, and rifaximin-bound peaks are shown in green. The number of ligand molecules bound to each β_2m monomer is depicted by the number of circles of each color above each peak. **d** ESI-IMS-MS Driftscope plot (IMS drift time *versus* m/z *versus* intensity (z = linear scale)) of β_2m incubated with 40 μM horse heart myoglobin and 40 μM rifamycin SV. Binding is observed only between β_2m and rifamycin SV (red circles). Analysis of the mass of β_2m in samples formed by mixing the protein with rifamycin S or rifamycin SV demonstrates that binding of the ligand to β_2m occurs without chemical modification of the protein (observed mass 11860±1 Da, mass expected of the wild-type protein is 11860 Da).

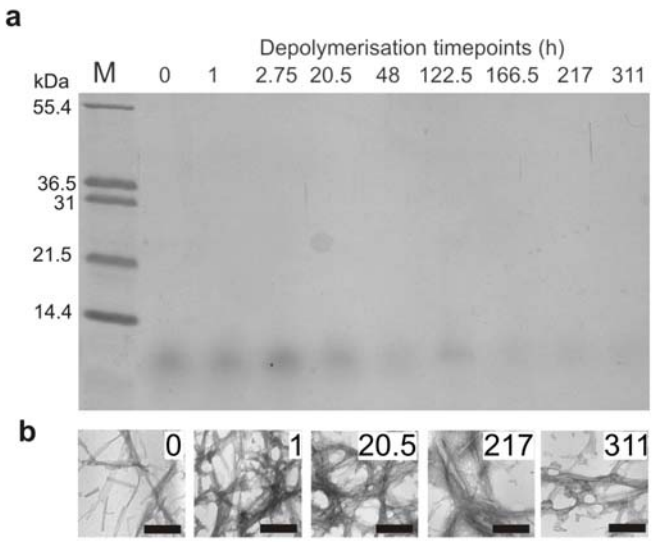

Supplementary Figure 3

Stability of LS fibrils formed from β_2m at pH 2.5 in the presence of rifamycin SV. **a** SDS-PAGE analysis of the supernatant following centrifugation of a sample of LS fibrils (formed from 45 μM β_2m monomer) incubated with 1 mM rifamycin SV at 25 ºC with agitation (600 rpm) for various times. **b** TEM images of a selection of the samples shown in **a**. The numbers on each image relate to the incubation time with rifamycin SV, in hours. The scale bar in each TEM image represents 200 nm.

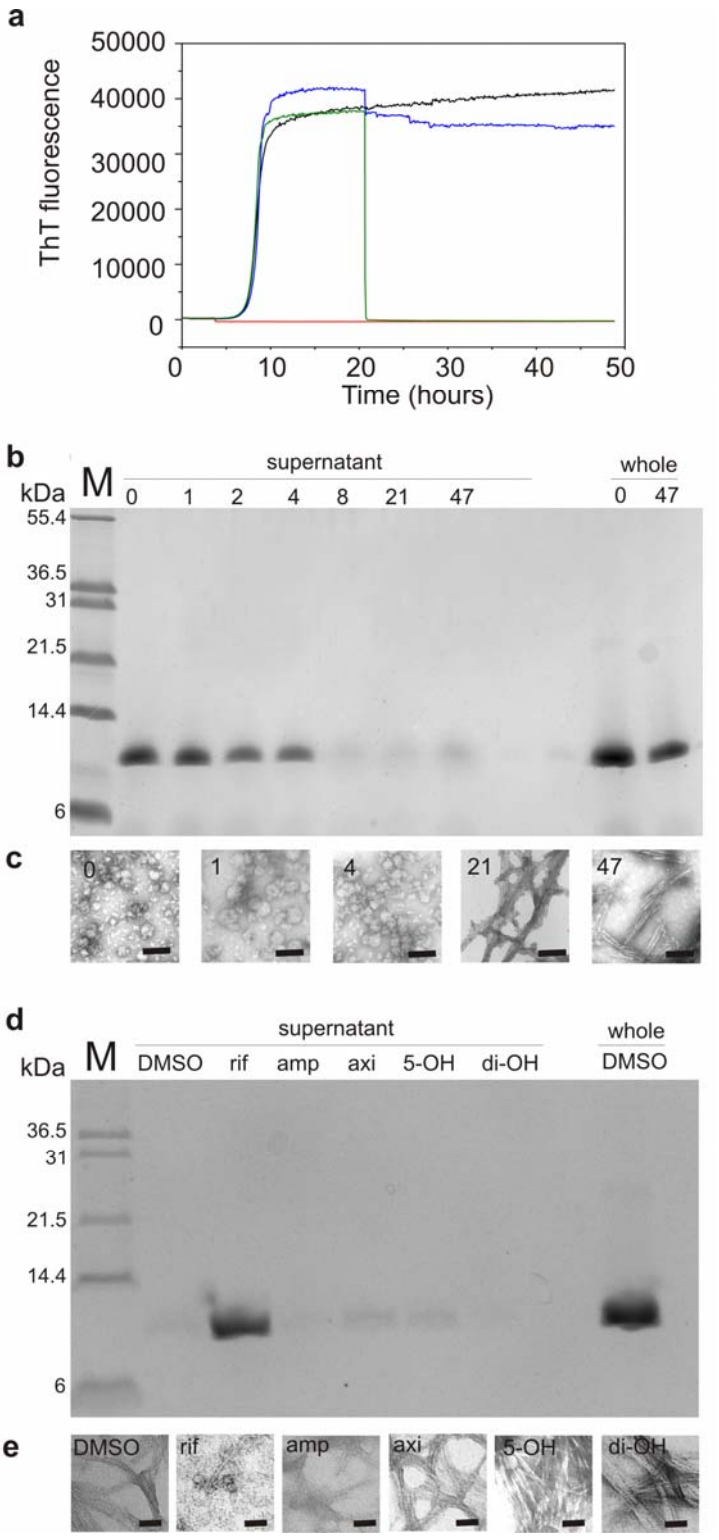

Supplementary Figure 4

Time-dependent effect of rifamycin SV on β_2m fibril formation. **a** ThT fluorescence of β_2m fibril assembly (45 μM monomer) showing experiments in which 10 % (*v/v*) DMSO alone was added to a fibril growth assay at t = 4 h (black) or at t = 21 h (blue). The small decrease in

signal in the latter is commensurate with dilution of the sample. Addition of 10 % (*v/v*) DMSO containing a final concentration of 1 mM rifamycin SV at t = 4 h (red) or at t = 21 h (green) is also shown. The lack of a ThT signal when rifamycin SV is added during the lag phase (t = 4 h) and the dramatic decrease in ThT fluorescence when rifamycin SV is added at t = 21 h results from displacement and/or quenching of ThT fluorescence by rifamycin SV. These traces nevertheless show the extent to which fibril formation had progressed before the ligand was added. **b** SDS-soluble material remaining after 48 h incubation of 45 μM β_2m at pH 2.5 with 1 mM rifamycin SV, with the small molecule added at the time points indicated (labeled 'supernatant (h)'). The total protein is shown for the experiment in which rifamycin SV was added at 0 or 47 h (labeled 'whole'). 10% (*v/v*) DMSO alone has no effect (< 5 %) on the proportion of soluble material remaining (not shown). **c** TEM images of the products of assembly, 48 h after adding rifamycin SV to fibril growth assays at 0, 1, 4, 8, 21 or 48 h of assembly (scale bar = 100 nm). **d** SDS-PAGE showing the soluble material remaining after seeded assembly of β_2m fibrils is complete (24h) (labeled supernatant) and the total protein concentration (labeled 'whole') for the reaction containing 10% (*v/v*) DMSO only. All assays contained 45 μM β_2m, 5% seed and 1 mM small molecule and were incubated at 25 ºC with agitation (600 rpm). Small molecules assayed are labeled as rif (rifamycin SV), amp (rifampicin), axi (rifaximin), 5-OH (5-hydroxy-1,4-naphthoquinone) and diOH (5,8-dihydroxy-1,4-naphthoquinone). **e** TEM images of the products of seeded assembly 24 h after incubation with the small molecule (scale bar = 100 nm).

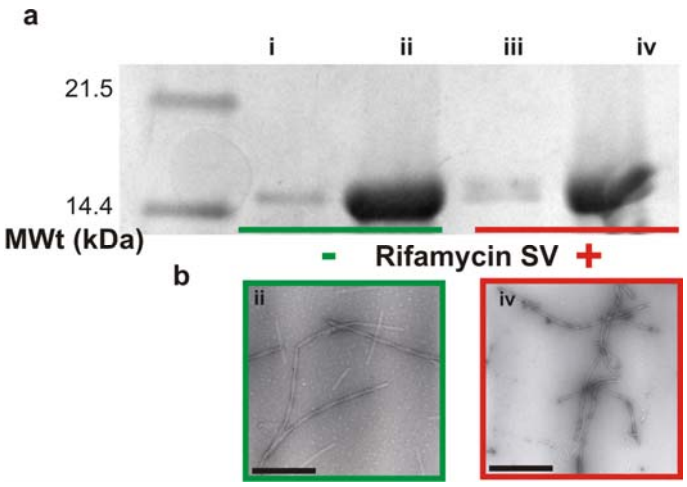

Supplementary Figure 5

Rifamycin SV does not inhibit α-synuclein fibrillation at pH 2.5. **a** SDS-PAGE analysis of SDS-soluble, low molecular weight material remaining after 72 h incubation of 69 μM α-synuclein in the presence or absence of 1 mM rifamycin. **i** and **iii** show the supernatant after centrifugation for 30 min at 16,300x *g*, showing little soluble α-synuclein remains when the protein is incubated in the absence or presence of rifamycin SV. **ii** and **iv** show the whole sample by SDS-PAGE. **b** TEM images of samples **ii** and i**v**. The scale bar in each TEM image represents 200 nm.

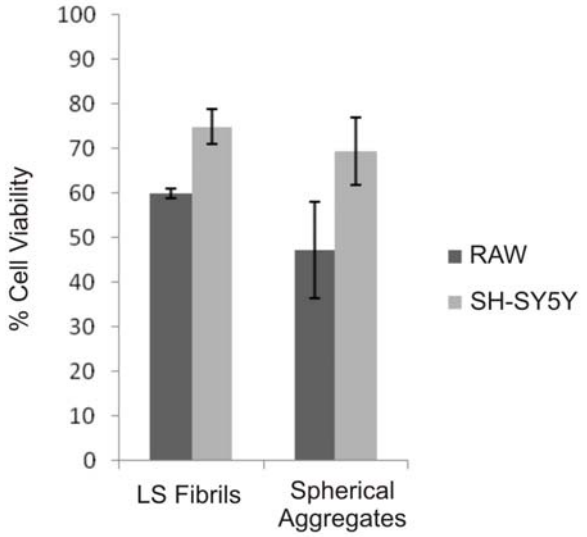

Supplementary Figure 6

Assays for cytotoxicity of different β_2m assemblies. RAW 264.7 (dark grey) or SH-SY5Y cells (light grey) were incubated with LS fibrils of β_2m fragmented by stirring at 1000 rpm for 24 h (mean length 366 nm), or oligomers formed by pre-incubation of β_2m monomers (for 48 h) with rifamycin SV. The toxicity of the assemblies formed was measured using the MTT assay (see Supplemental Methods). The data are normalized to cells incubated in buffer alone or buffer containing 1 mM rifamycin SV in 10 % (*v/v*) DMSO, diluted 1:100 into the culture medium, as appropriate. The error bars depict the standard error of the mean over three separate measurements.

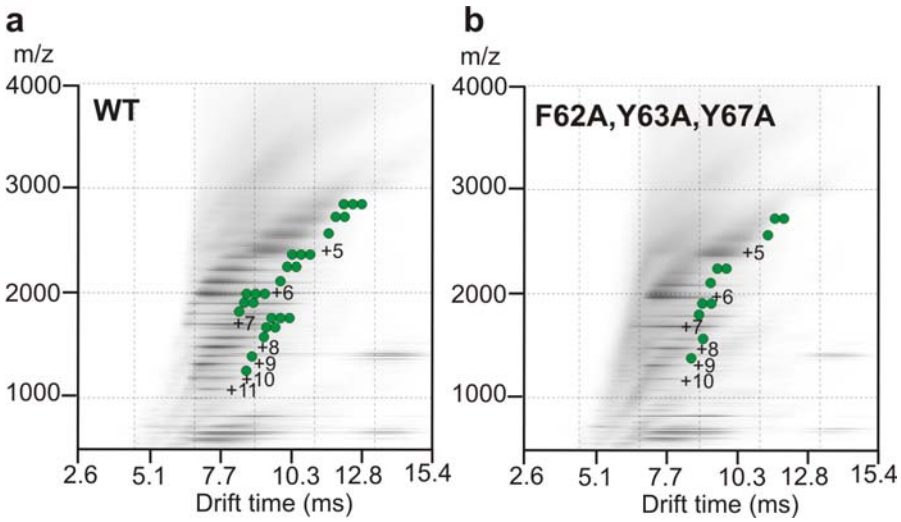

Supplementary Figure 7

ESI-IMS-MS Driftscope plots of monomeric β_2m in the presence of rifamycin SV. **a** Wild-type β_2m and rifamycin SV; **b** F62A,Y63A,F67A β_2m and rifamycin SV. All spectra were obtained at 25 ºC, pH 2.5 with β_2m (38 μM) dissolved in 10 mM ammonium formate and in the presence of an ~8-fold molar excess (320 μM) of rifamycin SV (dissolved in acetonitrile). The spectra (IMS drift time *versus* m/z *versus* intensity (z = square root scale)) were obtained within 2 min of ligand addition and the ESI-MS sampling cone voltage was set at 70 V (i.e., conditions optimised to monitor protein-ligand binding). The colored circles represent the number of ligand molecules bound to each charge state of β_2m in the different spectra.

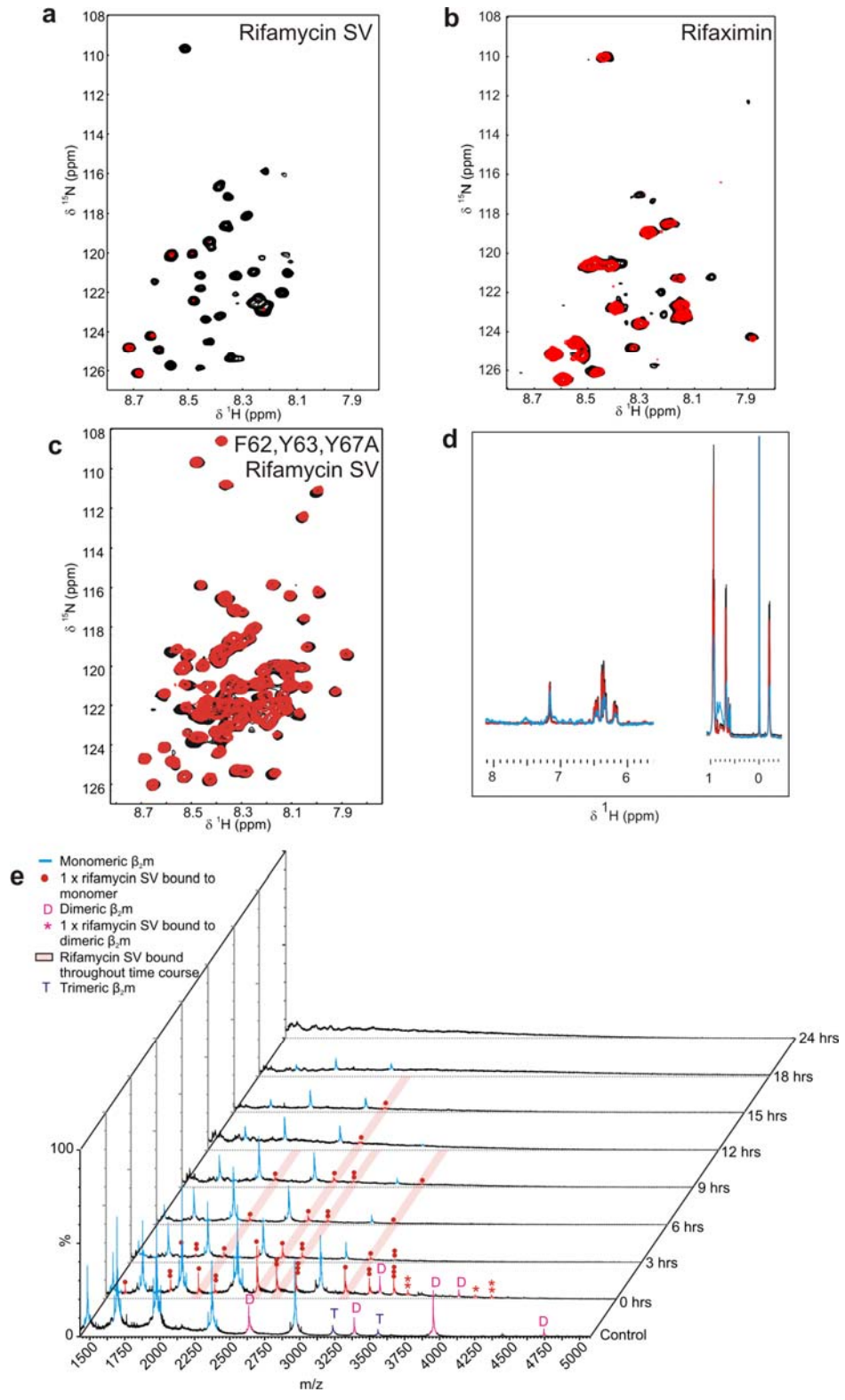

Supplementary Figure 8

Monomer signal depletes as rifamycin SV-induced spherical aggregates are formed. **a** ^{1}H-^{15}N HSQC NMR spectrum of 100 μM β_2m in 25 mM sodium phosphate, 25 mM sodium acetate

buffer (pH 2.5) in the absence (black) or presence (red) of 800 μM rifamycin SV. **b** ^{1}H-^{15}N HSQC NMR spectra of 100 μM β_2m in the absence (black) or presence (red) of 800 μM rifaximin. **c** ^{1}H-^{15}N HSQC NMR spectra of 100 μM F62A,Y63A,F67A in the absence (black) or presence (red) of 800 μM rifamycin SV. **d** ^{1}H 1D NMR spectra of 1 mM rifamycin SV in 25 mM sodium phosphate, 25 mM sodium acetate buffer (pH 2.5) in the presence of 0 μM (black), 5.9 μM (red) or 29.7 μM (blue) β_2m. The spectra are referenced and normalized to the peak for DSS. **e** ESI-MS spectra acquired at various time-points over 24 h after addition of 400 μM rifamycin SV to 38 μM β_2m. Over time the monomer ions deplete, presumably as large spherical aggregates form. These aggregates either do not ionize efficiently or are too diverse or large in mass to be detected under the conditions employed. In these spectra, blue peaks identify ligand free monomeric β_2m and rifamycin SV-bound peaks are shown in red. The number of ligand molecules bound to each β_2m monomer is depicted by the number of circles above each peak. Rifamycin SV remains bound to monomeric β_2m throughout the time course (highlighted by red bars). Dimeric and trimeric β_2m are labeled as “D” and “T”, respectively, and rifamycin SV bound to dimeric β_2m is depicted with red asterisks. Data were acquired at a sampling cone voltage of 170 V.

Molecule	**CAS reference**	LogD pH2	LogD pH7	LogP 25 °C	pKa	HB acceptor	HB donor
L-Tryptophan*	73-22-3	-1.76	-1.46	1.04 ± 0.12	1.10 ± 0.13 / 2.30 ± 0.1	4	4
L-Tyrosine*	60-18-4	-2.41	-2.12	0.38 ± 0.30	2.25 ± 0.10 / 9.35 ± 0.15	4	4
L-Phenylalanine*	63-91-2	-1.66	-1.39	1.11 ± 0.29	2.21 ± 0.10 / 9.20 ± 0.15	3	3
Tyramine*	51-67-2	-2.38	-1.98	0.72 ± 0.21	9.42 ± 0.26 / 10.63 ± 0.10	2	3
Curcumin*[†]	458-37-7	2.92	2.89	2.92 ± 0.48	8.09 ± 0.46	6	2
Rosmarinic acid*	20283-92-5	1.63	-1.93	1.70 ± 0.41	2.78 ± 0.1	8	5
Nordihydroguaiaretic acid (NDGA)*[†]	500-38-9	3.71	3.71	3.71 ± 0.26	9.56 ± 0.10	4	4
Epigallocatechin gallate (EGCG)*	989-51-5	2.08	2.01	2.08 ± 0.42	7.75 ± 0.25	11	8
Tannic acid**	1401-55-4						
Myricetin*	529-44-2	2.11	1.73	2.11 ± 0.74	6.89 ± 0.60	8	6
R(-)Apomorphine hydrochloride hemihydrates*	41372-20-7	-0.05	2.2	3.05 ± 0.40	7.88 ± 0.20 / 9.43 ± 0.20	3	2
L-DOPA**	59-92-7	-3.00	-2.73	-0.23 ± 0.32	2.24 ± 0.20 / 9.30 ± 0.3	5	5
Dopamine hydrochloride*	62-31-7	-2.98	-2.34	0.12 ± 0.22	9.39 ± 0.31 / 10.11 ± 0.1	3	4
6-Hydroxy-DOPA*	21373-30-8	-3.86	-3.55	-1.05 ± 0.38	2.34 ± 0.25 / 9.09 ± 0.43	6	6
5-Amino-2-methoxyphenol*	1687-53-2	-2.42	-0.07	-0.06 ± 0.23	4.91 ± 0.10 / 10.01 ± 0.1	3	3
3-Methoxy-L-tyrosine**	200630-46-2	-2.70	-2.42	0.08 ± 0.33	2.24 ± 0.20 / 9.30 ± 0.30	5	4
Guaiacol*	90-05-1	1.19	1.19	1.19 ± 0.22	9.97 ± 0.10	2	1
Resveratrol*	501-36-0	3.14	3.14	3.14 ± 0.34	9.15 ± 0.10	3	3
Ibuprofen*	15687-27-1	3.72	1.16	3.72 ± 0.23	4.41 ± 0.10	2	1
Naproxen*[†]	22204-53-1	3.00	0.85	3.00 ± 0.24	4.84 ± 0.30	3	1
2,2,2',2'-Tetrahydroxybenzophenone*	131-55-5	3.09	2.59	3.09 ± 0.42	6.98 ± 0.35	5	4
Clioquinol*	130-26-7	1.74	1.89	3.86 ± 0.83	2.10 ± 0.30 / 7.24 ± 0.59	2	1
Rifamycin SV Na salt*	14897-39-3	1.13	-0.43	1.53 ± 0.65	0.23 ± 0.70 / 5.17 ± 0.70	13	6
Rifaximin*	80621-81-4	2.65	0.4	3.22 ± 1.69	4.42 ± 0.70 / 8.06 ± 0.70	14	5
Rifampicin*	13292-46-1	-2.20	-1.28	1.07 ± 0.74	4.96 ± 0.70 / 7.30 ± 0.42	16	6
5,8-Dihydroxy-1,4-naphthoquinone*	475-38-7	1.82	1.73	1.82 ± 0.84	7.35 ± 0.20	4	2
5-Hydroxy-1,4-naphthoquinone*	481-39-0	1.86	1.53	1.86 ± 0.77	6.96 ± 0.20	3	1
o-Vanillin*	148-53-8	1.40	1.37	1.43 ± 0.28	8.17 ± 0.10	3	1
Neocuproine*	484-11-7	0.21	2.64	2.70 ± 0.23	6.16 ± 0.40	2	0
Lacmoid**	33869-21-5	1.72	3.16	3.18±1.48	3.68 ± 0.20/8.57 ± 0.40	8	6
Phenol red**	143-74-8	3.02	3.02	3.02 ± 0.42	9.01 ± 0.30	5	2
Apigenin*	520-36-5	2.10	1.83	2.10 ± 0.56	7.08 ± 0.40	5	3
Orange G**	1936-15-8						
Methylene blue**	7220-79-3						
Azure C**[†]	531-57-7						
Rolitetracycline**	751-97-3	-4.23	-3.06	-0.13 ± 0.84	4.50 ± 1.00 / 11.01 ± 0.70	11	6
Congo red*	573-58-0						
Thioflavin T**	2390-54-7						
Suramin*	129-46-4	-6.28	-6.30	2.194± 1.61	-1.35 ± 0.40 / -0.09 ± 0.50	29	12
Anthraquinone-2-sulfonic acid Na salt*[††]	131-08-8	-0.67	-1.01	2.49 ± 0.40	-1.42 ± 0.20	5	1
Quinizarin*	81-64-1	4.46	4.4	4.465 ± 0.77	7.54 ± 0.20	4	2
1-Aminoanthraquinone*	82-45-1	3.35	3.35	3.35 ± 0.62	-0.51 ± 0.20	3	2
Clarithromycin*	81103-11-9	0.06	1.98	3.16 ± 0.78	8.16 ± 0.70 / 13.08 ± 0.70	14	4
1-Pyrenebutyric acid*	3443-45-6	5.37	3.14	5.37 ± 0.20	4.76 ± 0.10	2	1

* ≥95% purity; ** purity unknown; [†] supplied by Fluka; [††]supplied by Alfa Aesar

Supplementary Table 1. Chemical properties of small molecules used in the screen. Data were obtained using SciFinder (www.cas.org/SCIFINDER/SCHOLAR/index.html). LogD is the logarithm of the partition coefficient between octanol and water at a given pH for the mixture of the neutral and ionic forms of a compound, calculated at 25 °C. LogP is the partition constant of neutral species under the same conditions. HB = hydrogen bond. Unless otherwise stated, all chemicals were supplied by Sigma Aldrich.

Molecule	Ref[a]	ThT Amp (%)[b]	ThT Lag[c]				Turbidity transition[d]	Soluble (%)[e]	TEM[f]
			<0.6x	NC	>1.5x	>2x			
L-Tryptophan		>50		✓			✓	<10	LS
L-Tyrosine		>50		✓			✓	<10	LS
L-Phenylalanine		>50		✓			✓	<10	LS
Tyramine		>50		✓			✓	<10	LS
Curcumin	17-22	0						<10	LS
Rosmarinic acid	17, 18, 20, 22	>20		✓			✓	<10	LS
Nordihydroguaiaretic acid (NDGA)	17-20	>50		✓			✓	<10	LS
Epigallocatechin gallate (EGCG)	17, 18, 21, 22	>20		✓			✓	<10	LS
Tannic acid	17, 18	>20			✓		✓	<30	LS, A
Myricetin	17-20, 22, 23	<20	✓					<10	LS
R(-)Apomorphine hydrochloride hemihydrate	17	>50		✓			✓	<10	LS
L-DOPA	24	>50		✓			✓	<10	LS
Dopamine hydrochloride	24	>50		✓			✓	<10	LS
6-Hydroxy-DOPA		<20		✓			✓	<10	LS
5-Amino-2-methoxyphenol		<20		✓			✓	<10	LS
3-Methoxy-L-tyrosine		>50		✓			✓	<10	LS
Guaiacol		>50		✓			✓	<10	LS
Resveratrol	17, 21	>20		✓			✓	<10	LS
Ibuprofen	25	>20		✓			✓	<10	LS
Naproxen	25	>50	✓				✓	<10	LS
2,2,2',2'-Tetrahydroxybenzophenone	17, 22, 23	>50		✓			✓	<10	LS
Clioquinol	26	<20		✓			✓	<10	LS
Rifamycin SV Na salt	19	0						>75	O, WL
Rifaximin		<20				✓		<10	LS, O
Rifampicin	18, 20, 22, 23, 27	<20			✓			<10	LS, O
Rifamycin S		<20				✓	✓	<50	LS, O
5,8-Dihydroxy-1,4-naphthoquinone	19	<20		✓			✓	<10	LS
5-Hydroxy-1,4-naphthoquinone	19	0					✓	<10	LS
o-Vanillin	19	>50		✓			✓	<10	LS
Neocuproine	19	>50		✓			✓	<10	LS
Lacmoid	19, 22, 23	0						<10	LS
Phenol red	19	0					✓	<10	A, LS
Apigenin	19, 22, 23	>20		✓			✓	<10	LS
Orange G	19	0						<10	A, O, LS
Methylene blue	22, 23	<20		✓				<10	LS
Azure C	19, 22, 23	<20			✓			<10	LS
Rolitetracycline	18, 19	>50		✓				<10	LS
Congo red	18, 19, 22, 27, 28	0						<10	LS, A
Thioflavin T	19	n/a					✓	<10	LS
Suramin	28	0						<10	WL, O
Anthraquinone-2-sulfonic acid		<20			✓		✓	<30	A, LS
Quinizarin		<20		✓			✓	<10	LS
1-Aminoanthraquinone		<20		✓			✓	<10	LS
Clarithromycin		>50		✓			✓	<10	LS
1-Pyrenebutyric acid		>20	✓				✓	<10	LS

Supplementary Table 2. Results of the screen for small molecule inhibitors of β_2m fibrillogenesis at pH 2.5. **a** Citations (and the references found therein) refer to studies in which the molecule listed was tested for modulation of protein aggregation reactions in different systems. **b** Final ThT signal amplitude (after incubation for 48 h) given as a percentage of a control reaction performed in parallel in the absence of each small molecule, but in the presence of 10 % (*v/v*) DMSO. **c** For reactions in which the small

molecule did not completely abolish ThT fluorescence the lag time of assembly was determined and is denoted in the table (with a tick) as either being reduced (<0.6-fold shorter lag time), not being changed (NC), being extended slightly (1.5-2.0-fold longer lag time) or being substantially extended (>2-fold longer lag time) compared with the lag time of a control reaction in the presence of 10 % (*v/v*) DMSO alone. Entries with no tick show reactions in which ThT fluorescence could not be monitored in the presence of the small molecule. **d** Fibril assembly was also monitored for each reaction using turbidity measurements at 635 nm. In the table a tick denotes a reaction in which a transition with lag-dependent kinetics indicative of fibril formation was observed. The absence of a tick is indicative of either lack of fibril formation or interference in the assay by the small molecule. **e** The percent soluble material remaining at the reaction endpoint (48 h) measured for each sample using centrifugation followed by analysis of the supernatant using SDS-PAGE (see Methods). **f** TEM images of each sample were examined (after 48 h) and classified as: A = amorphous aggregate, O = spherical aggregates, LS = long-straight fibrils, WL = worm-like fibrils.

Supplementary References

1. Lendel, C., *et al.* On the mechanism of nonspecific inhibitors of protein aggregation: Dissecting the interactions of α-synuclein with Congo red and lacmoid. *Biochemistry*, **48,** 8322-8334 (2009).

2. McGovern, S.L., Caselli, E., Grigorieff, N. and Shoichet, B.K. A common mechanism underlying promiscuous inhibitors from virtual and high-throughput screening. *J. Med. Chem.*, **45,** 1712-1722 (2002).

3. Feng, Y., *et al.* Resveratrol inhibits Aβ oligomeric cytotoxicity but does not prevent oligomer formation. *Neurotoxicology*, **30,** 986-995 (2009).

4. Feng, B.Y., *et al.* Small-molecule aggregates inhibit amyloid polymerization. *Nat. Chem. Biol.*, **4,** 197-199 (2008).

5. Mistrello, G., Cricchio, R., Bolzoni, G., Mosca, M. and Bassi, L. Immunogenicity of rifamycins. *Mol. Immunol.*, **16,** 665-669 (1979).

6. Uversky, V.N., Li, J. and Fink, A.L. Evidence for a partially folded intermediate in alpha-synuclein fibril formation. *J. Biol. Chem.*, **276,** 10737-10744 (2001).

7. Narhi, L., *et al.* Both familial Parkinson's disease mutations accelerate alpha-synuclein aggregation. *J. Biol. Chem.*, **274,** 9843-9846 (1999).

8. Cappai, R., *et al.* Dopamine promotes alpha-synuclein aggregation into sds-resistant soluble oligomers via a distinct folding pathway. *FASEB J.*, **19,** 1377-1379 (2005).

9. Xue, W.F., *et al.* Fibril fragmentation enhances amyloid cytotoxicity. *J. Biol. Chem.*, **284,** 34272-34282 (2009).

10. Meng, F.L., Marek, P., Potter, K.J., Verchere, C.B. and Raleigh, D.P. Rifampicin does not prevent amyloid fibril formation by human islet amyloid polypeptide but does inhibit fibril thioflavin-T interactions: Implications for mechanistic studies β-cell death. *Biochemistry*, **47,** 6016-6024 (2008).

11. Li, J., Zhu, M., Rajamani, S., Uversky, V.N. and Fink, A.L. Rifampicin inhibits α-synuclein fibrillation and disaggregates fibrils. *Chem. & Biol.*, **11,** 1513-1521 (2004).

12. Ferrige, A.G., *et al.* Disentangling electrospray spectra with maximum entropy. *Rapid Commun. Mass Spectrom.*, **6,** 707-711 (1992).

13. Sun, N., Sun, J., Kitova, E.N. and Klassen, J.S. Identifying non-specific ligand binding in electrospray ionization mass spectrometry using the reporter molecule method. *J. Am. Soc. Mass Spectrom.*, **20,** 1242-1250 (2009).

14. Sun, J., Kitova, E.N., Wang, W. and Klassen, J.S. Method for distinguishing specific from non-specific protein-ligand complexes in nanoelectrospray ionization mass spectrometry. *Anal. Chem.*, **78,** 3010-3018 (2006).

15. Smith, D.P., Giles, K., Bateman, R.H., Radford, S.E. and Ashcroft, A.E. Monitoring copopulated conformational states during protein folding events using electrospray ionization-ion mobility spectrometry-mass spectrometry. *J. Am. Soc. Mass Spectrom.*, **18,** 2180-2190 (2007).

16. Platt, G.W., Routledge, K.E., Homans, S.W. and Radford, S.E. Fibril growth kinetics reveal a region of β_2-microglobulin important for nucleation and elongation of aggregation. *J. Mol. Biol.*, **378,** 251-263 (2008).

17. Porat, Y., Abramowitz, A. and Gazit, E. Inhibition of amyloid fibril formation by polyphenols: Structural similarity and aromatic interactions as a common inhibition mechanism. *Chem. Biol. Drug Des.*, **67,** 27-37 (2006).

18. Hamaguchi, T., Ono, K. and Yamada, M. Anti-amyloidogenic therapies: Strategies for prevention and treatment of alzheimer's disease. *Cell. & Molec. Life Sci.*, **63,** 1538-1552 (2006).

19. Necula, M., Kayed, R., Milton, S. and Glabe, C.G. Small molecule inhibitors of aggregation indicate that Aβ oligomerization and fibrillization pathways are independent and distinct. *J. Biol. Chem.*, **282,** 10311-10324 (2007).

20. Shoval, H., Lichtenberg, D. and Gazit, E. The molecular mechanisms of the anti-amyloid effects of phenols. *Amyloid-J. of Protien Folding Disorders* **14,** 73-87 (2007).

21. Riviere, C., *et al.* Inhibitory activity of stilbenes on Alzheimer's Aβ fibrils *in vitro*. *Bioorg. & Med. Chem.*, **15,** 1160-1167 (2007).

22. Masuda, M., *et al.* Small molecule inhibitors of α-synuclein filament assembly. *Biochemistry*, **45,** 6085-6094 (2006).

23. Taniguchi, S., *et al.* Inhibition of heparin-induced tau filament formation by phenothiazines, polyphenols, and porphyrins. *J. Biol. Chem.*, **280,** 7614-7623 (2005).

24. Conway, K.A., Rochet, J.C., Bieganski, R.M. and Lansbury, P.T. Kinetic stabilization of the α-synuclein protofibril by a dopamine-α-synuclein adduct. *Science*, **294,** 1346-1349 (2001).

25. Hirohata, M., Ono, K., Morinaga, A. and Yamada, M. Non-steroidal anti-inflammatory drugs have potent anti-fibrillogenic and fibril-destabilizing effects for α-synuclein fibrils *in vitro*. *Neuropharmacology*, **54,** 620-627 (2008).

26. Nguyen, T., Hamby, A. and Massa, S.M. Clioquinol down-regulates mutant huntingtin expression *in vitro* and mitigates pathology in a huntington's disease mouse model. *Proc. Natl. Acad. Sci. USA*, **102,** 11840-11845 (2005).

27. Findeis, M.A. Approaches to discovery and characterization of inhibitors of Aβ-peptide polymerization. *Biochim. Biophys. Acta-Molecular Basis of Disease*, **1502,** 76-84 (2000).

28. Quaglia, M., *et al.* Search of ligands for the amyloidogenic protein β_2-microglobulin by capillary electrophoresis and other techniques. *Electrophoresis*, **26,** 4055-4063 (2005).